



Novel short-chain analogues of somatostatin as ligands for Cu(II) ions. Role of the metal ion binding on the spatial structure of the ligand

Aleksandra Marciniak^a, Marek Cebrat^b, Żaneta Czyżnikowska^a, Justyna Brasuń^{a,*}

^a Department of Inorganic Chemistry, Wrocław Medical University, Szewska 38, 50-139 Wrocław, Poland

^b Faculty of Chemistry, University of Wrocław, F. Joliot-Curie 14, 50-383, Wrocław, Poland

ARTICLE INFO

Article history:

Received 25 May 2012

Received in revised form 27 August 2012

Accepted 31 August 2012

Available online 7 September 2012

Keywords:

Somatostatin

Copper complexes

Histidine

Potentiometric measurements

Spectroscopic studies

Coordination

ABSTRACT

In this paper we present the studies on coordination abilities of two short-chain analogues of somatostatin with free N-terminal and protected amino group towards copper (II) ions. The octreotide is the most popular analogue of the somatostatin (peptide hormone) used in medicine. Somatostatin analogues are used in diagnosis and treatment of the neuroendocrine tumors. Both analyzed analogues are characterized by the presence of two His instead of Cys residues in characteristic fragment of native peptide. We characterize coordination abilities of the ligands using potentiometric and spectroscopic methods. His-analogues of somatostatin are effective ligands for copper (II) ions. Both peptides are able to form the complexes with the cyclic structure.

© 2012 Elsevier Inc. All rights reserved.

1. Introduction

Somatostatin (SST) is a peptide hormone existing in the human body which takes part in the regulation of endocrine system and affects neurotransmission and cell proliferation via interaction with somatostatin receptors and inhibition of numerous secondary hormones [1].

The native somatostatin exists in two forms which differ in length of the peptide chain. The first one is formed by 14 while the second one by 28 amino acid residues, respectively [1]. Nevertheless, both peptides have the same cyclic motif in their structures. This motif is formed by the disulfide bridge between Cys and Cys residues. The characteristic feature of the SST peptides is also the presence of the –PheTrpLysThr–sequence [1] (Scheme 1a). The native SST hormone has a short half-life (about 2 min) in the body. The analogues with longer half-lives are used in medicine and they are very promising tool in therapy and diagnosis.

The octreotide (OCT) is the most popular analogue of the somatostatin used in medicine, e.g. the [¹¹¹In-DTPA]-octreotide was used for the scintigraphy of the neuroendocrine tumors [2]. This peptide is characterized by the DPhe-c (Cys-Phe-DTrp-Lys-Thr-Cys)-Thr-ol sequence [3].

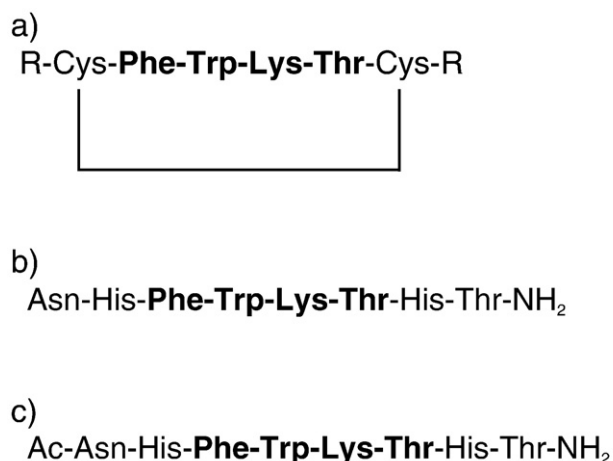
The somatostatin analogues are used in scintigraphy, targeted chemo- and radiotherapy. The presence of somatostatin receptors in tumor cells causes that somatostatin analogues could be used in visualization and detection of tumors, in control of hormonal hypersecretion and tumor growth [4]. In the future new analogues of somatostatin with high affinity for different somatostatin receptors should be developed. The study of various radionuclides is also desirable [5].

The previous studies on coordination abilities of His-analogues of vasopressin and oxytocin have shown that insertion of two His amino acid residues instead of Cys causes huge increase of efficacy in metal ion coordination. Moreover, both analogues form the cyclic complex with the {NH₂, N[−], N_{im(macrochelate)}}} binding mode in the physiological range of pH [6]. These results allow us to perform studies on binding abilities of His-analogues of somatostatin with copper (II) ion. The copper was chosen due to the fact that its isotope, ⁶⁴Cu, is an attractive radionuclide for PET imaging and radiotherapy [7,8]. Previous studies show that ⁶⁴Cu-TETA-OCT could be used as a PET imaging agent for patients with neuroendocrine tumors [9].

In this paper we present studies performed for two short-chain analogues of somatostatin with free and protected N-terminal amino group (Scheme 1b,c). Both analogues are characterized by the presence of two His instead of Cys residues in characteristic fragment of native peptide. The replacement of both Cys by His residues causes loss of the cyclic motif in the peptide structure and also insertion of effective donor atoms for the metal ions, especially for copper. The

* Corresponding author. Fax: +48 71 784 03 36.

E-mail address: justyna.brasun@am.wroc.pl (J. Brasuń).



Scheme 1. Structure of peptides: a) characteristic fragment of somatostatin and its analogues, b) NH₂-[His^{2,7}]P1, c) Ac-[His^{2,7}]P2.

analysis of the potentiometric together with spectroscopic results allows us to characterize the binding abilities of investigated ligands. We performed also molecular modeling investigations in order to determine the possible structures of formed complexes.

2. Materials and methods

2.1. Synthesis of the peptides

Peptides were synthesized by the standard manual Fmoc (9-Fluorenylmethoxycarbonyl) solid-phase peptide synthesis method on the Fmoc-Rink Amide MBHA resin (0.65 mM/g, Iris Biotech GmbH). Synthesis was carried out in single-use plastic reactors (Intavis GmbH). The following amino acid derivatives were used for the synthesis: Fmoc-Thr (tBu)-OH, Fmoc-His (Trt)-OH, Fmoc-Lys (Boc)-OH, Fmoc-Trp (Boc)-OH, Fmoc-Phe-OH, and Fmoc-Asn (Trt)-OH (Boc – t-butoxycarbonyl, Trt – triphenylmethyl). Subsequent Fmoc-protected amino acids (3 eq) were attached by using 3 eq TCTU (O-(6-Chlorobenzotriazol-1-yl)-N,N,N',N'-tetramethyluronium tetrafluoroborate) as a coupling reagent in the presence of N-hydroxybenzotriazole (3 eq) and diisopropylethylamine (6 eq) for 2 h at room temperature. Fmoc protecting groups were removed by 25% piperidine in dimethylformamide. Acetylation of the N-terminal amino group was achieved on the resin by 1:1 mixture of acetic anhydride and 0.4 M N-methylmorpholine in dimethylformamide. Final cleavage of the peptides was achieved by “Reagent K” (81.5% trifluoroacetic acid, 5% phenol, 5% thioanisole, 5% water, 2.5% ethanedithiol, 1% triisopropylsilane) in 2 h at room temperature. Crude peptides were precipitated by cold diethylether, washed with ether, dissolved in water and lyophilized.

Peptides were purified by semipreparative HPLC using Varian ProStar apparatus equipped with TOSOH Bioscience C18 column (300 Å, 21.5 mm, 10 µm beads) and 220 nm UV detector. Water–acetonitrile gradients containing 0.1% TFA (trifluoroacetic acid) at a flow rate of 7 mL/min were used for the purifications. Final purity

of the lyophilized peptides was >97% by analytical HPLC (Thermo Separation Product; column: Vydac Protein RP C18, 250 Å 4.6 mm, 5 µm; linear gradient 0–100% B in 60 min, solvent A – 0.1% TFA in water, solvent B – 0.1% TFA in 80% acetonitrile:water solution, UV detection at 220 nm). Chemical identity of the ligands was confirmed by ESI-MS on a Bruker micrOTOF-Q mass spectrometer. Analytical data of the synthesized peptides are given in Table 1.

2.2. Potentiometric measurements

Potentiometric measurements were carried out using Molspin pH-meter system with a Mettler Toledo InLab 422 semimicro combined electrode at 25 °C calibrated in hydrogen ion concentration using HCl [10]. The ligand concentration was 8×10^{-4} M and pH-metric titrations were performed in 0.1 M KCl using sample volumes of 1.2 mL. Alkali was added by using a 0.25 mL micrometer syringe. Stability constants and stoichiometry of the complexes were calculated from titration curves using SUPERQUAD program [11].

2.3. Spectroscopic measurements

Visible spectra of complexes were recorded on Varian Carry 50 Bio spectrophotometer. The EPR spectra were recorded on Bruker ELEXSYS E500 CW-EPR, X-Band spectrometer, equipped with ER 036TM NMR Teslameter and E 41 FC frequency counter. Circular dichroism (CD) spectra were recorded on a JASCO J 600 spectropolarimeter in 300–800 nm range. The same concentrations were used for both spectroscopic and potentiometric studies.

2.4. Fluorescence measurements

Fluorescence measurements were performed with Cary Eclipse fluorescence spectrophotometers using 280 nm excitations for both N-protected and unprotected derivative of octreotide containing tryptophane. The fluorescence spectra were recorded using 8×10^{-5} M peptide solutions at 25 °C. The titration was performed at fixed pH 7 and pH 11.5 as a function of metal concentration. The measurements were performed for pure ligands and ligand–metal ratios in the range of 1:0.1–1:8.7.

2.5. Molecular modeling

The geometry optimizations of all complexes were carried out taking into account solvent effects using the continuum PCM model at the B3LYP/6-31G (d) level of theory [12,13]. Harmonic frequency analysis was performed to verify that the structures correspond to a stationary point on the potential energy surface. The previous study on the coordination abilities of peptides have confirmed that this level of theoretical approximation may provide reliable description of structural as well as energetic properties for bioinorganic complexes [14]. Molecular modeling was performed with the aid of the Gaussian 09 program [15].

Table 1
Analytical data of the peptides.

Peptide	[M + H] ⁺		[M + H] ²⁺		R _t ^c [min]	Preparative gradient ^d
	Calc. ^a	Found ^b	Calc. ^a	Found ^b		
NH ₂ -[His ^{2,7}]P1	1069.533	1069.531	535.270	535.521	17.25	15–25% B in 45 min
Ac-[His ^{2,7}]P2	1111.543	1111.544	556.275	556.28	16.54	15–23% B in 45 min

^a Monoisotopic mass calculated for the indicated ion formed by the peptide.

^b Monoisotopic mass found by ESI-MS.

^c Retention time of the crude peptide found by analytical HPLC.

^d HPLC gradient used for the semipreparative purification of the peptides.

3. Results

3.1. The coordination abilities of the $\text{NH}_2\text{-[His}^{2,7}\text{]P1}$

Stability constants for proton and complexes of copper are collected in Table 2. The studied peptide has four protonation constants assigned to both His ($\text{p}K=5.56$ and 6.24), free N-terminal amino group ($\text{p}K=6.87$) and Lys ($\text{p}K=10.12$) amino acid residues and they are comparable to the protonation constants of these groups found in the literature [16].

The $\text{NH}_2\text{-[His}^{2,7}\text{]P1}$ starts copper coordination around pH 3 which is manifested by the formation of the CuHL species with the highest concentration around pH 4 (Fig. 1). The EPR parameters ($A_{\parallel}=189$ [G], $g_{\parallel}=2.229$, Table 2) obtained at pH 4 strongly support binding of three nitrogen atoms to the metal ion [17]. There are two main possibilities of formation of 3N complex by this peptide: with -NH_2 , $\text{N}_{\text{Im}2}$, $\text{N}^-_{\text{amide}}$ or -NH_2 , $\text{N}_{\text{Im}2}$, $\text{N}_{\text{Im}7(\text{macrochelate})}$ binding modes. The first type of coordination is characteristic for the peptides with XaaHis motif [18–20] while the second one was observed in the case of di-His-analogues of

peptide hormones [6]. The value of $\log\beta^* \approx 6$ of the discussed complex is comparable to the one calculated for the 3N complex with -NH_2 , $\text{N}^-_{\text{amide}}$, N_{Im} chromophores ($\log\beta_{\text{CuHL-1L}} \approx 5.5\text{--}6$) [21–23], where $\log\beta^* = \log\beta_{\text{CuHL}} - (\text{p}K_{\text{Lys}} + \text{p}K_{\text{His}})$. It supports the -NH_2 , N_{Im} , $\text{N}^-_{\text{amide}}$ atoms as donors in the CuHL complex. This assumption is also supported by comparison of the experimental value of λ_{max} for d–d transition with the theoretical value of λ_{max} calculated for these chromophores. The value of λ_{max} for d–d transition in absorption spectrum occurs at 596 nm and corresponds more to the -NH_2 , N_{Im} , $\text{N}^-_{\text{amide}}$, H_2O donor sets with the $\lambda_{\text{max}(\text{theoretical})} = 599$ nm than to the -NH_2 , N_{Im} , $\text{N}_{\text{Im}(\text{macrochelate})}$, H_2O donor sets with $\lambda_{\text{max}(\text{theoretical})} = 625$ nm [24,25].

Above pH 4 the CuL complex appears in the system and dominates up to pH 9 (Fig. 1). Blue shift of λ_{max} for d–d transition in absorption spectrum (≈ 30 nm) to $\lambda_{\text{max}} = 567$ nm strongly supports binding of next nitrogen to metal ion. The EPR parameters obtained for the system at pH 7.5 ($A_{\parallel} = 200$ [G] and $g_{\parallel} = 2.211$) confirm coordination of four nitrogens to metal ion [26]. There are two options: i/ binding of the amide nitrogen of Phe³ amino acid residue and formation of the

Table 2
Stability constants of H^+ and Cu (II)-peptide complexes with $\text{NH}_2\text{-[His}^{2,7}\text{]P1}$ and $\text{Ac-[His}^{2,7}\text{]P2}$ and the spectroscopic parameters at 25 °C, $I=0.1$ M (KCl).

		$\log \beta$	$\text{p}K$	UV–VIS		EPR		CD	
				λ (nm)	E ($\text{M}^{-1} \text{cm}^{-1}$)	A_{\parallel} (G)	g_{\parallel}	λ (nm)	$\Delta\epsilon$ ($\text{M}^{-1} \text{cm}^{-1}$)
$\text{NH}_2\text{-[His}^{2,7}\text{]P1}$	HL	10.12 ± 0.03							
	H_2L	16.99 ± 0.05							
	H_3L	23.23 ± 0.04							
	H_4L	28.79 ± 0.05							
	$\text{p}K_{\text{Lys}}^*$		10.12						
	$\text{p}K_{\text{NH}_2}^*$		6.87						
	$\text{p}K_{\text{His}}^*$		6.24						
	$\text{p}K_{\text{His}}^*$		5.56						
	CuHL	21.68 ± 0.01		596	50	189	2.229	605 ^a 358 ^c 309 ^b	0.23 0.053 –0.19
	CuL	16.47 ± 0.01		567	67	200	2.211	568 ^a 482 ^a 343 ^c 300 ^b	0.096 –0.089 0.043 –0.18
	CuH_{-1}L	6.88 ± 0.02		–	–	–	–	–	–
	CuH_{-2}L	-3.45 ± 0.02		–	–	–	–	–	–
	CuH_{-3}L	-14.55 ± 0.02		525	107	202	2.208	510 ^a 324 ^c	–0.32 0.12
	$\text{p}K_{\text{CuHL-CuL}}^{**}$		5.21						
	$\text{p}K_{\text{CuL-CuH}_{-1}\text{L}}^{**}$		9.59						
	$\text{p}K_{\text{CuH}_{-1}\text{L-CuH}_{-2}\text{L}}^{**}$		10.33						
$\text{p}K_{\text{CuH}_{-2}\text{L-CuH}_{-3}\text{L}}^{**}$		11.10							
$\text{Ac-[His}^{2,7}\text{]P2}$	HL	10.01 ± 0.01							
	H_2L	16.59 ± 0.03							
	H_3L	22.41 ± 0.03							
	$\text{p}K_{\text{Lys}}^*$		10.01						
	$\text{p}K_{\text{His}}^*$		6.58						
	$\text{p}K_{\text{His}}^*$		5.82						
	CuHL	15.32 ± 0.01		689	20	164	2.279	–	–
	CuL	8.89 ± 0.02		–	–	–	–	–	–
	CuH_{-1}L	2.49 ± 0.01		587	54	183	2.222	583 ^a 365 ^c 327 ^b	–0.17 –0.071 0.059
	CuH_{-2}L	-5.72 ± 0.02		514 590	65 Sh	198	2.182	632 ^a 490 ^a 352 ^c 318 ^c	0.31 –0.88 –0.17 0.28
	$\text{p}K_{\text{CuHL-CuL}}^{**}$		6.43						
	$\text{p}K_{\text{CuL-CuH}_{-1}\text{L}}^{**}$		6.40						
	$\text{p}K_{\text{CuH}_{-1}\text{L-CuH}_{-2}\text{L}}^{**}$		8.21						
	$\text{p}K_{\text{CuH}_{-2}\text{L-CuH}_{-3}\text{L}}^{**}$		10.64						

^a d–d transition.

^b $\text{N}_{\text{Im}} \rightarrow \text{Cu(II)}$ CT.

^c $\text{N}^- \rightarrow \text{Cu(II)}$ CT.

* $\text{p}K_{\text{N}} = \log\beta_{\text{Hn}+1} - \log\beta_{\text{Hn}}$.

** $\text{p}K_{\text{N}} = \log\beta_{\text{CuHn}+1\text{L}} - \log\beta_{\text{CuHn-1L}}$.

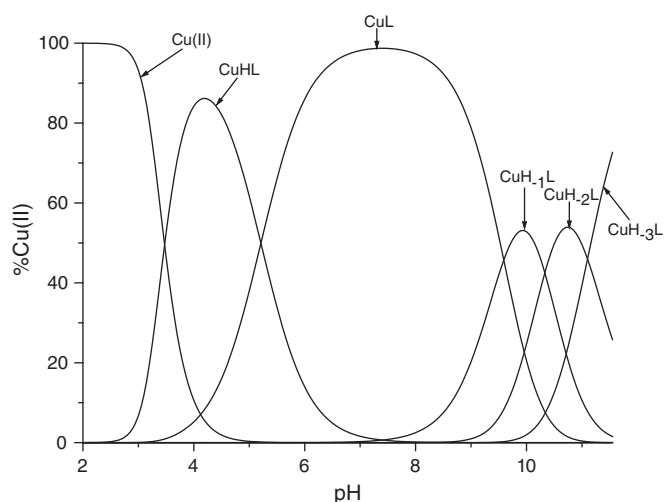


Fig. 1. Potentiometric profile of $\text{NH}_2\text{-[His}^{2,7}\text{]P1}$ copper (II) complexes; ligand concentration 8×10^{-4} mol/l; metal to ligand ratio 1:1; $I = 0.1$ M (KCl).

species with the $\{\text{NH}_2, 2\text{xN}^-_{\text{amide}}, \text{N}_{\text{im}2}\}$ binding mode or ii/ coordination of the imidazole nitrogen from His⁷ and formation of the complex with $\{\text{NH}_2, \text{N}^-_{\text{amide}}, \text{N}_{\text{im}2}, \text{N}_{\text{im}7}\}$ chromophores. The involvement of the second amide nitrogen should influence significantly the CD spectrum between 300 and 350 nm where CT (charge transfer) transitions $\text{N}^- \rightarrow \text{Cu(II)}$ are observed. In the analyzed system this effect is not observed (Fig. 2, Table 1) and the second, $\{\text{NH}_2, \text{N}^-_{\text{amide}}, \text{N}_{\text{im}2}, \text{N}_{\text{im}7}\}$, coordination mode can be proposed.

As pH increases other three complexes, namely CuH_{-1}L , CuH_{-2}L and CuH_{-3}L , appear in the system (Fig. 1, Table 1) but spectroscopic parameters could be obtained only for the last, CuH_{-3}L , complex. The appearance of this species causes significant changes in the spectroscopic abilities of the system, especially in the CD spectrum (Fig. 2, Table 1). The blue shift of λ_{max} for d-d transition to 525 nm and the appearance of positive CT transition at 324 nm show major involvement of amide nitrogens in metal ion binding. Due to these facts the amino and three amide nitrogen chromophores in square planar complexes can be proposed for the CuH_{-3}L species.

3.2. The coordination abilities of the $\text{Ac-[His}^{2,7}\text{]P2}$

The protection of the N-terminal amino group affects the $\text{Ac-[His}^{2,7}\text{]P2}$ that has one protonation constant less. The other three

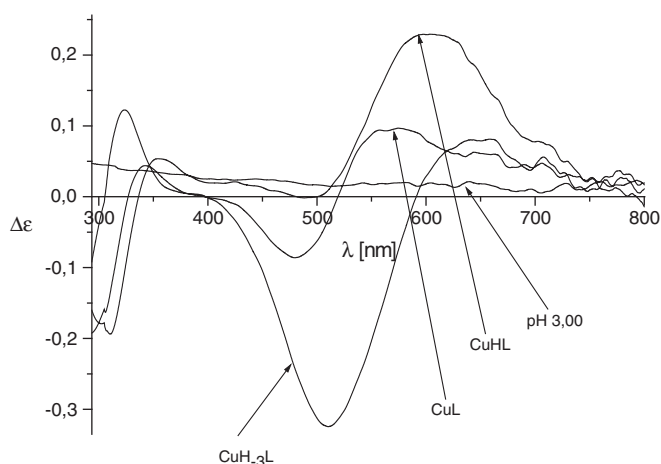


Fig. 2. CD spectra of $\text{Cu(II)/NH}_2\text{-[His}^{2,7}\text{]P1}$ solutions at different pH levels.

constants for both His and Lys are comparable to the calculated constant for the unprotected peptide (Table 2).

Protection of the N-terminal amino group significantly changes the coordination abilities of the peptide. The studied $\text{Ac-[His}^{2,7}\text{]P2}$ starts copper (II) binding by formation of the CuHL (Fig. 3) species similarly to its unprotected analogue. However, the spectroscopic parameters suggest 2N coordination (Table 2). The value of λ_{max} at 689 nm (Table 2) strongly supports the binding of two imidazole nitrogens of both His residues [25]. Due to this process the created complex has a cyclic structure. Above pH 6 the other two protons dissociate from the discussed complex and the CuL together with CuH_{-1}L complexes appears in the system. The CuL complex has the highest concentration at pH 6.5 where the CuHL and CuH_{-1}L complexes exist in comparable concentrations. Therefore determination of the spectroscopic parameters for this species was too difficult to carry out. Appearance of the CuH_{-1}L form causes a blue shift of λ_{max} in absorption spectrum (to 587 nm, Table 2). The experimental value of λ_{max} is in good agreement with the theoretical $\lambda_{\text{max}} = 584$ nm calculated for the two amides, one imidazole nitrogen and one oxygen from water molecule donor sets [25] and EPR parameters ($A_{\text{H}} = 183$ [G], $g_{\text{H}} = 2.222$, Table 2) confirm coordination of three nitrogens to Cu (II). Involvement of amide and imidazole nitrogens in metal ion coordination is supported by the presence of two CT bands: negative at 365 nm and positive at 327 nm (Table 2). The studied peptide has two His residues in its sequence: in the 2nd and 7th positions. It starts copper binding by both His (CuHL species). Then involvement of amide nitrogens is observed. In the literature it can be found that His amino acid residue promotes coordination of its peptidic nitrogen [27]. Due to this fact the $\{\text{N}_{\text{im}7}, \text{N}^-_{\text{amide of His7}}, \text{N}^-_{\text{amide of Thr6}}\}$ binding mode can be proposed.

Formation of the next CuH_{-2}L complex causes significant changes in the spectroscopic parameters. The blue shift of λ_{max} in the absorption spectrum together with the increase of EPR parameters (Table 2) suggests binding of four nitrogens to the metal ion. The pK value of proton dissociation and formation of this complex is equal to 8.21 and supports binding of the next amide nitrogen and formation of the square planar complex with the $\{\text{N}_{\text{im}}, 3 \times \text{N}^-_{\text{amide}}\}$ binding mode [28].

Finally, the CuH_{-3}L complex is created in the systems and dominates above pH 11. The value of pK for proton dissociation and formation of this complex ($\text{pK} = 10.64$) and any significant changes in the spectroscopic parameters suggest proton dissociation from the Lys residue. This has no impact on binding of the metal ion.

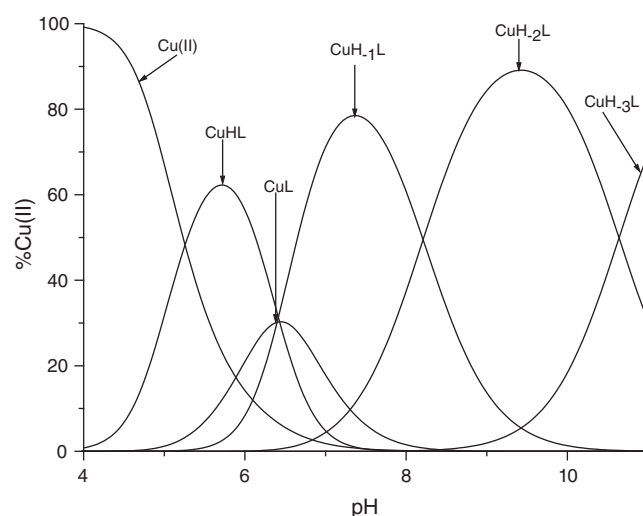


Fig. 3. Potentiometric profile of $\text{Ac-[His}^{2,7}\text{]P2}$ copper (II) complexes; ligand concentration 8×10^{-4} M; metal to ligand ratio 1:1; $I = 0.1$ M (KCl).

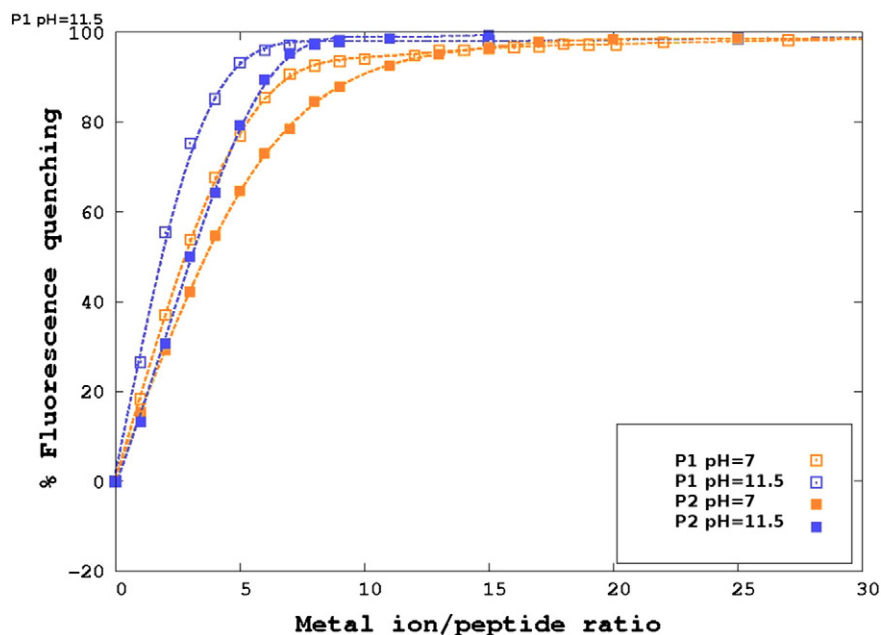


Fig 4. Fluorescence quenching of investigated complex in the presence of increasing concentrations.

3.3. The structural aspects of Cu (II) binding

3.3.1. Fluorescence measurements

Both investigated ligands contain aromatic amino acids, phenylalanine and tryptophan which are responsible for the fluorescence emission in proteins. Interpretation of peptide fluorescence in the presence of multiple fluorescent amino acids is a very complicated task. However, in the considered cases the absorption and emission spectra of tryptophan residue overlap the spectra of phenylalanine. In both considered pH, namely 7 and 11.5 the emission maxima of 360 nm are typical for tryptophan fluorophore. Due to the tendency of excited-state indole to donate electrons Trp appears to be uniquely sensitive to collisional quenching. Many reports on this subject have been recorded in the literature [29–31]. As far as the coordination abilities of Ac-[His^{2,7}]P2 are concerned at pH=7 CuH₋₁L species dominates in the solution with {H₂O, N_{lm}, 2 N^{-amide}} binding mode.

Moreover, in the case of NH₂-[His^{2,7}]P1 at the same value of pH the CuL species is formed. At pH=11.5 N-protected derivative of octreotide forms CuH-L stable complex characterized by {N_{lm}, 3 N^{-amide}} binding mode. As far as Ac-[His^{2,7}]P2 pure ligand is concerned the maximum of fluorescence intensities are equal to 10.71 and 11.72 for pH 7 and pH 11, respectively. The intensity of fluorescence for NH₂-[His^{2,7}]P1 at pH 7 is almost the same, on the other hand at pH 11.5 the intensity is smaller by about 50%. Quenching of N-protected and N-terminal free derivatives of ligand fluorescence by increasing concentrations of copper presented in Fig. 4 follows hyperbolic curve. In the case Ac-[His^{2,7}]P2 at pH 7 and pH11.5 and NH₂-[His^{2,7}]P1 at neutral pH after adding the first portion of copper (peptide/metal ratio 1:0.1) lower than 20% fluorescence quenching is observed. In alkaline 25% fluorescence quenching for NH₂-[His^{2,7}]P1 is noticed after adding the same amount of Cu (II). For ligand/metal ratio 1:0.4 fluorescence quenching increases by about 50% in the case of both Ac-[His^{2,7}]P2 and NH₂-[His^{2,7}]P1 in neutral

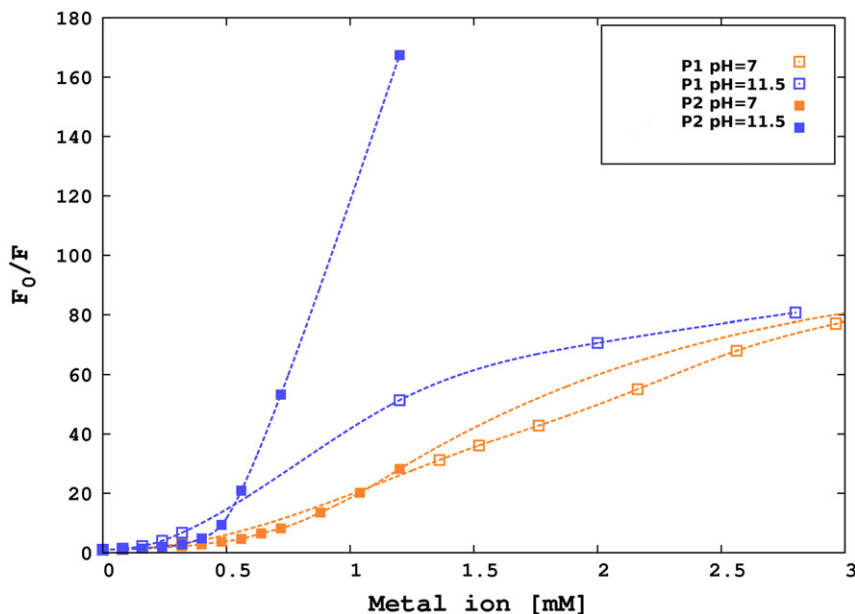


Fig 5. Stern-Volmer plot for copper (II) quenching of $8 \cdot 10^{-5}$ M solution of investigated complex.

and alkaline solutions. As far as Ac-[His^{2,7}]P2 and NH₂-[His^{2,7}]P1 peptides are concerned, fluorescence quenching is almost 100% for peptide/metal ratio 1:1.2. The fluorescence quenching of investigated peptides allows determination of the extent of fluorophore (tryptophan) exposure to the aqueous solution. To better understand the quenching mechanism during titration of peptides with Cu (II) ions, the data were analyzed using Stern–Volmer equation [32]:

$$F_0/F = 1 + K_{SV}[Q],$$

where F_0 and F are fluorescence intensities in the absence and presence of copper, respectively. The K_{SV} is the Stern–Volmer constant, and $[Q]$ is the concentration of the metal ion [32]. Constant appearing in the above equation indicates the sensitivity of ligand to the quencher. The plotted curves (Fig. 5) for quenching by Cu (II) at both considered pH show upward curvature which is indicative for complex (static vs dynamic) quenching mechanism. The first type of quenching is induced by formation of nonfluorescent complex while the latter is connected with collisions arising from diffusive encounters between fluorophore and quenchers. The obtained data indicate that aromatic tryptophan residue is not buried inside the peptide but on the surface of the created complexes in both considered pH. However, in the case of CuL complex of NH₂-[His^{2,7}]P1 and CuH₋₁L complex of Ac-[His^{2,7}]P2, aromatic ring of tryptophan is located closer to the peptide chain. It is in agreement to our molecular modeling findings.

3.3.2. Molecular modeling study

In order to analyze the structural aspects of the binding properties of short-chain analogues of somatostatin towards copper ions we performed quantum chemical calculations. The initial set of plausible conformations of the complexes of ligands with Cu (II) at different pH levels (in total around 30 structures) were optimized at PM6 level of theory leading to many unique conformations. The most energetically favored conformations (i.e. those of the lowest total energy including zero-point energy) were reoptimized using the B3LYP functional. In this paragraph, we report only on the most stable conformers of complexes with cyclic structures. Fig. 6 contains the lowest-energy structures of Cu (II)–peptide complexes obtained based on quantum-chemical calculations. The structural parameters, namely Cu (II)–N distances vary from 1.9 to 2.2 Å which is in agreement with data obtained from X-ray diffraction measurements collected in CSD (Cambridge Structural Database) database [33].

As far as CuHL species for N-protected peptide is concerned, it is found that the metal ion is coordinated by two nitrogen atoms of histidine moieties. We analyzed also the structure of tetra coordinated complex of N-terminal free derivative of octerotide. Contrary to Ac-[His^{2,7}]P2 ligand, the N-terminal part of NH₂-[His^{2,7}]P1 is involved in copper coordination. This peptide is found to bind Cu (II) in the CuL protonation state. In this case metal is coordinated by two imidazoles, first amide and amino group nitrogens.

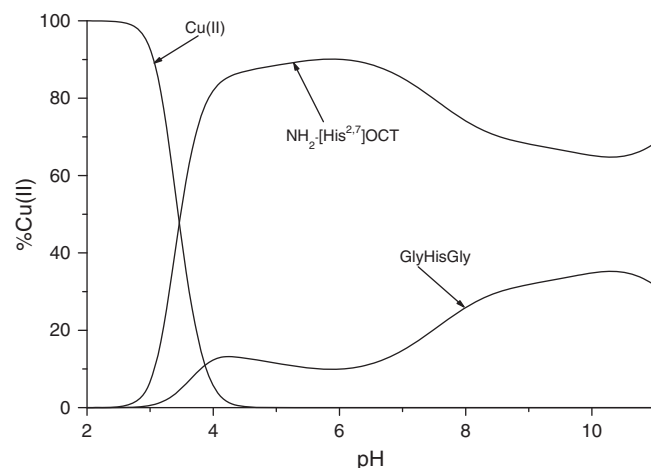


Fig. 7. Comparison of the efficacy of copper (II) binding between GlyHisGly and NH₂-[His^{2,7}]P1.

4. Discussion

Figs. 7, 8 and 9 show the competition diagrams of the ligand1/Cu (II)/ligand2 systems. These types of diagrams allow comparison of the efficiency in metal ion binding between two ligands. It allows obtaining of the quantity of bounded metal ions by ligand1 and by ligand2 in each pH.

Fig. 7 shows the competition diagram for system NH₂-[His^{2,7}]P1/Cu (II)/Gly-His-Gly [18].

The investigated NH₂-[His^{2,7}]P1 starts copper coordination in the same way as Gly-His-Gly [18] peptide by formation of the first complex with the {NH₂, N⁻_{amide}, N_{Im2}} binding mode. Nevertheless, this ligand is much more effective in Cu (II) binding than the simple tripeptide. The significant higher efficiency in Cu (II) coordination of the NH₂-[His^{2,7}]P1 can be explained by the fact that the investigated peptide forms stable four nitrogen complexes with the {NH₂, N⁻_{amide}, N_{Im2}, N_{Im7}(macrochelate)} binding mode already above pH 5.5 while in the same range of pH the Gly-His-Gly forms still 3N complex with the NH₂, N⁻_{amide}, and N_{Im2} chromophores.

The comparisons of the efficiency in Cu (II) binding between the protected ligand, Ac-[His^{2,7}]P2, and similar protected peptides are presented in Figs. 8 and 9. Fig. 8 shows the comparison of analyzed peptide with AcGlyHisGlyGly [28] because this peptide has His residue in the position 2 of the peptide chain. In Fig. 9 are compared Ac-[His^{2,7}]P2 and AcGlyGlyGlyHis [28] because both of them form the same type of complexes. As it can be seen in both considered cases the protected analogue of somatostatin is much more effective in copper coordination. The reason for the higher efficiency in metal binding by the investigated peptide is probably the same as in the

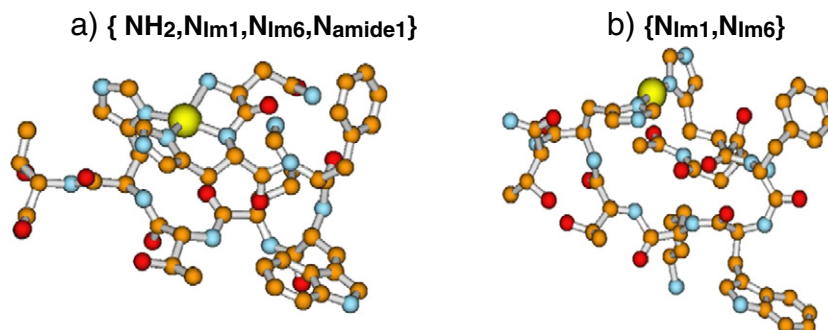


Fig. 6. Structures of investigated cyclic complexes of NH₂-[His^{2,7}]P1 (a) and Ac-[His^{2,7}]P2 (b). The data were obtained at the 6–31 G (d) level of theory.

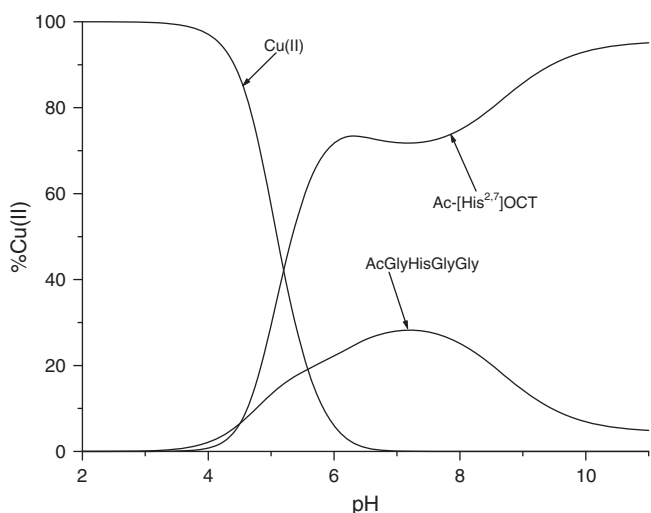


Fig. 8. Comparison of the efficacy of copper (II) binding between AcGlyHisGlyGly and Ac-[His^{2,7}]P2.

previously discussed system (unprotected peptide). The presence of two histidines and formation of the complex with cyclic structure significantly facilitate the process of Cu (II) binding.

As it was shown above, studied peptides are able to form complexes with cyclic structure: CuL (in a case of NH₂-[His^{2,7}]P1) and CuHL (in a case of Ac-[His^{2,7}]P2). In order to determine the effects of somatostatin modifications on the structural properties of aromatic fragments of NH₂-[His^{2,7}]P1 and Ac-[His^{2,7}]P2 the optimal geometries of NH₂-[Cys^{2,7}]P1 and Ac-[Cys^{2,7}]P2 were found.

The comparison of aromatic part of complexes and Cys-analogues of analyzed peptides structures shows that the modification of N-protected peptide does not causes significant changes in the arrangement of aromatic amino acid rings phenylalanine and tryptophan (see Fig. 10).

5. Conclusions

In the presented paper we have shown that the His-analogues of octreotide are effective ligands for Cu (II) ions. In the basic conditions they form stable four nitrogen complexes with three amide nitrogens bound to the metal ion. The most interesting is that both peptides are able to form the complexes with the cyclic structures. The comparison

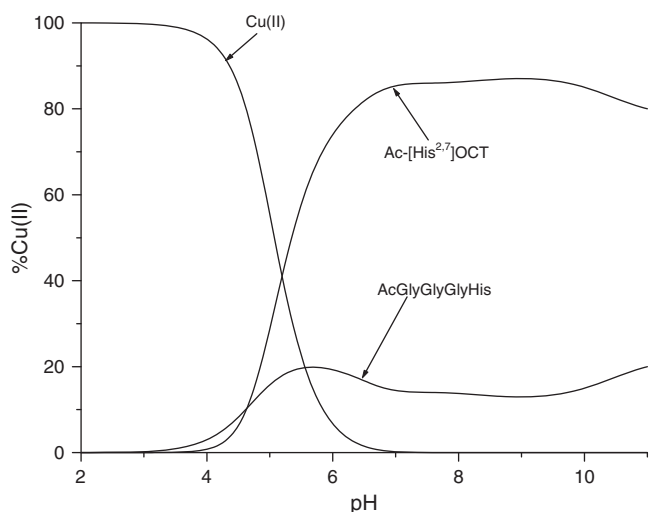


Fig. 9. Comparison of the efficacy of copper (II) binding between AcGlyGlyGlyHis and Ac-[His^{2,7}]P2.

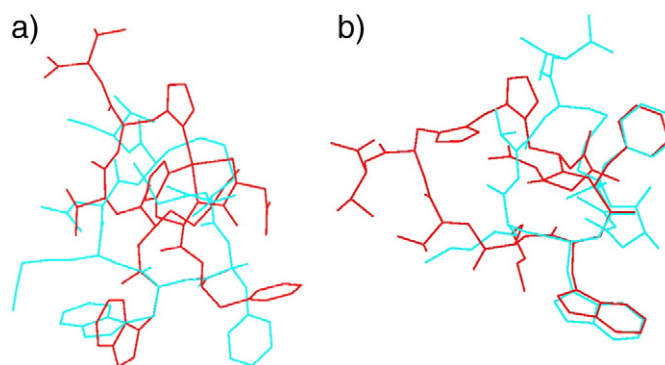


Fig. 10. The comparison of the calculated structures of the Cys-analogues of analyzed peptides (blue) and a) CuL complex for NH₂-[His^{2,7}]P1, b) CuHL complex for Ac-[His^{2,7}]P2 with the cyclic structures (red).

of structures of the mentioned complexes and structure of their Cys-analogues has shown that the location of the aromatic rings of Phe and Trp is very similar in the case of protected peptide however the whole structure of the part with the –Phe-Trp-Lys-Thr-sequence is not strictly the same.

Acknowledgements

Authors gratefully acknowledge the allotment of the CPU time in Wrocław Center of Networking and Supercomputing (WCSS).

References

- [1] Y.C. Patel, *Front. Neuroendocrinol.* 20 (1999) 157–198.
- [2] K. Chen, P.S. Conti, *Adv. Drug Deliv. Rev.* 62 (2010) 1005–1022.
- [3] J. Strosberg, L. Kvols, *World J. Gastroenterol.* 16 (2010) 2963–2970.
- [4] S.W.J. Lamberts, W.W. de Herder, L.J. Hofland, *Trends Endocrinol. Metab.* 13 (2002) 451–457.
- [5] J.J.M. Teunissen, D.J. Kwekkeboom, M. de Jong, J.P. Esser, R. Valkema, E.P. Krenning, *Best Pract. Res. Clin. Gastroenterol.* 19 (2005) 595–616.
- [6] J. Brasuń, M. Cebrat, Ł. Jaremko, M. Jaremko, G. Ilc, O. Gładysz, Igor Zhukov, *Dalton Trans.* (2009) 4853–4857.
- [7] C.L. Ferreira, D.T. Yapp, E. Lamsa, M. Gleave, C. Bensimon, P. Jurek, G.E. Kiefer, *Nucl. Med. Biol.* 35 (2008) 875–882.
- [8] J.S. Lewis, M.R. Lewis, P.D. Cutler, A. Srinivasan, M.A. Schmidt, S.W. Schwarz, M.M. Morris, J.P. Miller, C.J. Anderson, *Clin. Cancer Res.* 5 (1999) 3608–3616.
- [9] C.J. Anderson, F. Dehdashti, P.D. Cutler, S.W. Schwarz, R. Laforest, L.A. Bass, J.S. Lewis, D.W. McCarthy, *J. Nucl. Med.* 42 (2001) 213–221.
- [10] H.M. Irving, M.G. Miles, L.D. Pettitt, *Anal. Chim. Acta* 38 (1967) 475–488.
- [11] P. Gans, A. Sabatini, A. Vacca, SUPERQUAD: an improved general program for computation of formation constants from potentiometric data, *J. Chem. Soc. Dalton Trans.* (1985) 1195–1200.
- [12] E. Cancès, B. Mennucci, J. Tomasi, *J. Chem. Phys.* 107 (1997) 3032–3041.
- [13] J. Tomasi, B. Mennucci, E.J. Cancès, *J. Mol. Struct. THEOCHEM* 464 (1999) 211–226.
- [14] J.P. Stewart James, *J. Mol. Model.* 15 (2009) 765–805.
- [15] M.J. Frisch, G.W. Trucks, H.B. Schlegel, G.E. Scuseria, M.A. Robb, J.R. Cheeseman, G. Scalmani, V. Barone, B. Mennucci, G.A. Petersson, H. Nakatsuji, M. Caricato, X. Li, H.P. Hratchian, A.F. Izmaylov, J. Bloino, G. Zheng, J.L. Sonnenberg, M. Hada, M. Ehara, K. Toyota, R. Fukuda, J. Hasegawa, M. Ishida, T. Nakajima, Y. Honda, O. Kitao, H. Nakai, T. Vreven, J.A. Montgomery Jr., J.E. Peralta, F. Ogliaro, M. Bearpark, J.J. Heyd, E. Brothers, K.N. Kudin, V.N. Staroverov, R. Kobayashi, J. Normand, K. Raghavachari, A. Rendell, J.C. Burant, S.S. Iyengar, J. Tomasi, M. Cossi, N. Rega, J.M. Millam, M. Klene, J.E. Knox, J.B. Cross, V. Bakken, C. Adamo, J. Jaramillo, R. Gomperts, R.E. Stratmann, O. Yazyev, A.J. Austin, R. Cammi, C. Pomelli, J.W. Ochterski, R.L. Martin, K. Morokuma, V.G. Zakrzewski, G.A. Voth, P. Salvador, J.J. Dannenberg, S. Dapprich, A.D. Daniels, Ö. Farkas, J.B. Foresman, J.V. Ortiz, J. Cioslowski, D.J. Fox, *Gaussian 09, Revision A.1*, Gaussian, Inc., Wallingford CT, 2009.
- [16] R.H. Holm, P. Kennepohl, E.I. Solomon, *Chem. Rev.* 96 (1996) 2239–2314.
- [17] F.E. Mabbs, D. Collins, in: *Studies in Inorganic Chemistry, Electron of the peptide itself, Paramagnetic Resonance of d-Transition Metal Compounds*, Vol. 12, Elsevier, Amsterdam, 1992.
- [18] S. Bruni, F. Cariati, P.G. Daniele, E. Prenesti, *Spectrochim Acta A* 56 (2000) 815–827.
- [19] H. Kozłowski, T. Kowalik-Jankowska, M. Jeżowska-Bojczuk, *Coord. Chem. Rev.* 249 (2005) 2323–2334.
- [20] H. Kozłowski, W. Bal, M. Dyba, T. Kowalik-Jankowska, *Coord. Chem. Rev.* 184 (1999) 319–346.

- [21] Ch. Conato, R. Gavioli, R. Guerrini, H. Kozłowski, P. Mlynarz, C. Pasti, F. Pulidori, M. Remelli, *Biochem. Biophys. Acta* 1526 (2001) 199–210.
- [22] P.G. Daniele, O. Zerbinati, V. Zelano, G. Ostacoli, *J. Chem. Soc. Dalton Trans.* (1991) 2711–2715.
- [23] N.I. Jakab, B. Gyurcsik, T. Körtvélyesi, I. Vosekalna, J. Jensen, E. Larsen, *J. Inorg. Biochem.* 101 (2007) 1376–1385.
- [24] E.J. Billo, *Inorg. Nucl. Chem. Lett.* 10 (1974) 613–617.
- [25] E. Prenesti, P.G. Daniele, M. Principe, G. Ostacoli, *Polyhedron* 18 (1999) 3233–3241.
- [26] J. Peisach, W.E. Blumberg, *Arch. Biochem. Biophys.* 165 (1974) 691–708.
- [27] H. Siegel, R.B. Martin, *Chem. Rev.* 82 (1982) 385–426.
- [28] M. Orfei, M.C. Alcaro, G. Marcon, M. Chelli, M. Ginnaneschi, H. Kozłowski, J. Brasun, L. Messori, *Biochem* 97 (2003) 299–307.
- [29] S.S. Lehrer, *Biochem.* 10 (1971) 3254–3263.
- [30] T.A. Wells, M. Nakazawa, K. Manabe, P.S. Song, *Biochem.* 33 (1994) 708–712.
- [31] P. Midoux, P. Wahl, J.C. Auchet, M. Monsigny, *Biochim. Biophys. Acta* 801 (1984) 16–25.
- [32] J.R. Lakowicz, in: *Principles of fluorescence spectroscopy*, Third Edition, Kluwer Academic Publisher, 2006, pp. 238–259.
- [33] F.H. Allen, O. Kennard, R. Taylor, *Acc. Chem. Res.* 16 (1983) 146–153.